forests

MDPI

Article

Comparative Chloroplast Genome Analysis of Chinese Lacquer Tree (*Toxicodendron vernicifluum*, Anacardiaceae): East-West Divergence within Its Range in China

Lu Wang [1], Yao Li [1], Na He [2], Ye Peng [1], Yanming Fang [1,*], Xingwang Zhang [3,*] and Feilong Zhang [2]

[1] Co-Innovation Center for Sustainable Forestry in Southern China, Key Laboratory of State Forestry and Grassland Administration on Subtropical Forest Biodiversity Conservation, College of Biology and the Environment, Nanjing Forestry University, 159 Longpan Road, Nanjing 210037, China
[2] Xi'an Raw Lacquer Research Institute, 1 Tiantan Road, Xi'an 710061, China
[3] School of Life Sciences, Huaibei Normal University, 100 Dongshan Road, Huaibei 235000, China
* Correspondence: jwu4@njfu.edu.cn (Y.F.); zhangxingwang79@126.com (X.Z.)

Abstract: Chinese lacquer tree (*Toxicodendron vernicifluum*) is an important commercial arbor species known for the production of raw lacquer. Here, we investigated the intraspecific chloroplast (cp) genome variability of *T. vernicifluum* using two available and five newly sequenced cp genomes. We found that each of the seven cp genomes encoded 87 protein-coding genes, 37 tRNA genes, and eight rRNA genes. Phylogenetic analyses based on protein-coding genes indicated that the four individuals from western China formed a monophyletic group sister to the cluster containing the three individuals from eastern China. The cp genomes from western China exhibited a larger genome length and longer large single-copy (LSC), small single-copy (SSC), and inverted repeat (IR) regions than those from eastern China. A total of 466 single nucleotide polymorphisms (SNPs) and 141 insertion-deletion mutations were detected among the seven cp genomes, most of which were found between the eastern and western lineages. The two groups exhibited a similar number of microsatellites, long repeats, and tandem repeats. Notably, complementary repeat sequences were only found in the IRs of the individuals from eastern China, while reverse repeat sequences were only detected in the LSC of the individuals from western China. Eight intraspecific mutational hotspots were also identified, including six intergenic regions (*trnF-ndhJ*, *rpl32-trnL*, *ccsA-ndhD*, *trnH-psbA*, *psbC-trnS*, and *trnL-trnF*) and two gene regions (*rpl32* and *rps19*). The genomic resources presented in this study will be useful for further studies on evolutionary patterns and resource protection of *T. vernicifluum*.

Keywords: chloroplast; phylogeny; phylogeographic structure; SNPs; *Toxicodendron vernicifluum*

Citation: Wang, L.; Li, Y.; He, N.; Peng, Y.; Fang, Y.; Zhang, X.; Zhang, F. Comparative Chloroplast Genome Analysis of Chinese Lacquer Tree (*Toxicodendron vernicifluum*, Anacardiaceae): East-West Divergence within Its Range in China. *Forests* **2023**, *14*, 818. https://doi.org/10.3390/f14040818

Academic Editor: David Lee

Received: 19 February 2023
Revised: 3 April 2023
Accepted: 12 April 2023
Published: 17 April 2023

1. Introduction

Toxicodendron vernicifluum (Stokes) F. A. Barkley, commonly known as the Chinese lacquer tree, is a deciduous and dioecious tree species in the sumac family Anacardiaceae. This species is famous for providing us with raw lacquer, an excellent binder, and painting material with various properties such as anti-corrosion, rust resistance, non-oxidation, acid resistance, alcohol resistance, and high-temperature resistance [1,2]. In addition, *T. vernicifluum* is an economic tree species that is sometimes used in Chinese medicine to treat internal parasites and to stop bleeding. Previous studies have also reported that the urushiols of this species may have anticancer activity against human cancer cells and that flavonoids extracted from its leaves have therapeutic potential as a multipotent agent to treat neurodegenerative diseases [3,4].

T. vernicifluum is naturally distributed in China and has been cultivated in Korea and Japan perhaps for thousands of years [2,5,6]. In western China, wild lacquer trees usually grow in mountainous areas with an altitude above 800 m (e.g., the Qinling Mountains,

the Daba Mountains, the Wuling Mountains, the Dalou Mountains, and the Wumeng Mountains). In eastern China, they are scattered in low-altitude areas (e.g., the Liaodong Peninsula, the Shandong Peninsula, and the Huangshan Mountains). By analyzing the sequence variation of two chloroplast (cp) DNA fragments (*trnL* and *trnL-F*), previous studies have shown that *T. vernicifluum* exhibited a clear east-west phylogeographic break that was associated with the stepped geomorphology of China [1,7]. The wild trees of the western lineage were mainly found in the "middle step" region that is characterized by high mountains and plateaus, while those of the eastern lineage were confined to the "low step" region that is made up of hills and plains. These findings suggested that *T. vernicifluum* may have undergone allopatric divergence between at least two glacial refugia [7].

Compared with a few sequence fragments, complete cp genomes contain a larger amount of phylogenetic information, often used for phylogenetic inference and species delimitation [8–10]. Cp genomes are more conserved than mitochondrial and nuclear genomes in terms of gene content, organization, and structure [11–13]. With the development of bioinformatics and high-throughput sequencing technologies, the value of cp genomes in understanding evolutionary biology and ecological applications has been widely recognized [14–16]. However, it should also be noted that interspecific cpDNA sharing is also frequently observed among co-occurring, closely related species (e.g., *Quercus*, *Populus*, and *Eucalyptus*) as a result of introgression (secondary contact) or shared geographic origin (ancestral sympatry) [17–19]. Thus, it is essential to use information from as many closely related species as possible to track the evolutionary history of cpDNA lineages.

The genus *Toxicodendron* included about 20 species, of which 16 are distributed in China [20]. In the last four years, cp genomes of several *Toxicodendron* species have been reported [21–23]. Comparative analyses of cp genomes were also reported for the genus *Toxicodendron* and other genera of Anacardiaceae, such as *Cotinus* [24], *Mangifera* [25], *Pistacia* [26,27], and *Rhus* [28]. For example, Barrett [29] exhibited an interesting finding that the gene rps19 was lost independently in the *Rhus integrifolia-ovata* complex and *R. chinensis*, with a further loss of the gene rps22 and a major contraction of the inverted repeat in two accessions of the latter. At the intraspecific level, Xu et al. [28] have detected obvious differences in cp genome length and the lengths of the large single-copy (LSC) and inverted repeat (IR) regions among four individuals of *R. chinensis*. The cp genomes of those individuals also varied in the numbers of protein-coding genes (126–132) and tRNA genes (36–37).

Recently, Zong et al. [30] compared the cp genomes of triploid *T. vernicifluum* and several cultivars of the species. They found that the size of those cp genomes varied but the structure and organization of genes were conservative. However, this study did not investigate the cp genome variation of natural populations of *T. vernicifluum*. Our present study particularly focused on the intraspecific cp genome variability of wild trees of *T. vernicifluum* sampled from its natural range in China. Given that previous studies using two cpDNA fragments have revealed an east-west phylogeographic split of *T. vernicifluum* associated with the stepped geomorphology of China [7], we hypothesized that there were significant differences between cp genomes of the species sampled from its western and eastern range in China. Here, we assembled and annotated the cp genomes of two *T. vernicifluum* trees from western China and three trees from eastern China and compared them with those previously reported (Figure 1). The observed patterns were also compared with the results based on nuclear ribosomal internal transcribed spacer (ITS) variation. We purposed to: (1) evaluate the genetic relationships of *T. vernicifluum* accessions using both cp genome and ITS variation; (2) investigate the intraspecific cp genome variability of *T. vernicifluum* between its eastern and western range in China; (3) explore potential variable regions useful for phylogeographic studies of *T. vernicifluum*.

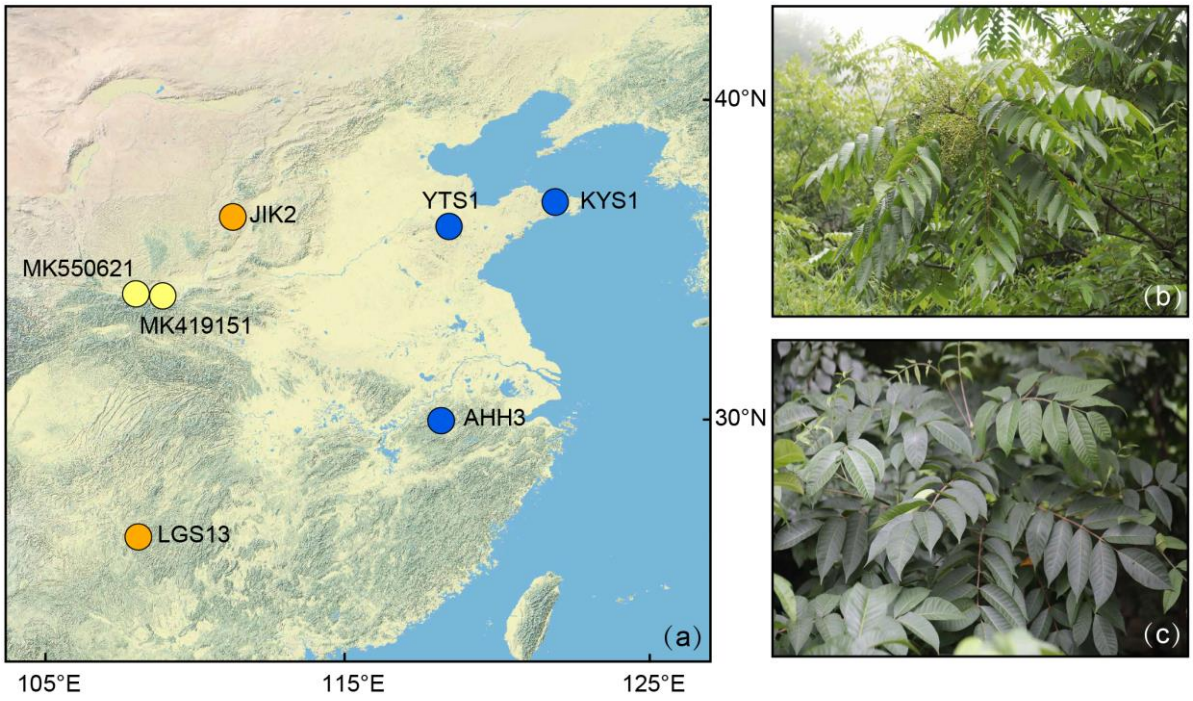

Figure 1. (**a**) Sampling sites of the seven *Toxicodendron vernicifluum* trees. The blue, orange, and yellow circles represent the three newly sequenced trees sampled from eastern China (voucher number: YTS1, KYS1, and AHH3), the two newly sequenced trees sampled from western China (voucher number: JIK2 and LGS13), and the two previously sequenced trees sampled from western China (GenBank accession number: MK419151 and MK550621), respectively. (**b**) Leaf photo of the individual sampled from western China (LGS13). (**c**) Leaf photo of the individual sampled from eastern China (KYS1). All photos were taken by Lu Wang.

2. Materials and Methods

2.1. Sampling, DNA Extraction, and Sequencing

Between July 2019 and August 2021, we sampled healthy and fresh leaves of five wild trees of *T. vernicifluum* from two sites in western China (voucher numbers: JIK2 and LGS13) and three sites in eastern China (voucher numbers: YTS1, KYS1, and AHH3) (Figure 1 and Table S1). Spatially explicit information was recorded for each tree using the 2bulu Outdoor Assistant app (https://www.2bulu.com/) (accessed on 25 June 2021). The voucher specimens of the five individuals were stored at the Herbarium of Nanjing Forestry University (NF) under voucher numbers shown in Table S1. Total genomic DNA was extracted from silica-gel dried leaves using the cetyltrimethylammonium bromide (CTAB) method [31]. The DNA integrity was evaluated with 1% agarose gel electrophoresis. The DNA concentration was measured by an ultra-micro ultraviolet-visible spectrophotometer (One Drop, Beijing, China). Qualified DNA samples were sent to Beijing Genomics Institute (BGI, Wuhan, China) for paired-end library preparation and whole-genome sequencing on a DNB-SEQ platform. Raw reads were filtered and trimmed using SOAPnuke 2.1.7 [32] with the following parameters: -n 0.01-l 20-q 0.3–adaMR 0.25–ada_trim–polyX 50–minReadLen 150.

2.2. Chloroplast Genome Assembly and Annotation

Paired-end clean reads were used for the de novo assembly of the five cp genomes with GetOrganelle 1.7.6.1 [33], which exploits SPAdes [34], Bowtie2 [35], BLAST+ [36], and Bandage [37] as dependencies. A wide range of k-mer lengths (-k 21, 45, 65, 85, 105) was used to benefit from the power of SPAdes. The maximum extension rounds (-R) were set to 15. The CpGAVAS2 pipeline [38] was applied to annotate protein-coding, rRNA, and tRNA genes using *T. vernicifluum* 'Dahongpao' (GenBank accession number:

MK550621) as the reference sequence. The Chloroplast Genome Viewer (CPGView) online tool (http://www.1kmpg.cn/cpgview) (accessed on 1 January 2023) [39] was used to visualize the cp genome structures.

2.3. Phylogenetic Analyses and Divergence Time Estimation Based on Chloroplast Genome Sequences

Twenty-three cp genomes were used to reconstruct the phylogeny of the tribe Rhoeae (Table 1). Those plastomes belonged to five species of the genus *Toxicodendron* (11 plastomes), six species of the genus *Rhus* (seven plastomes), one species of the genus *Cotinus* (one plastome), and three species of the genus *Pistacia* (three plastomes). *Mangifera indica* (GenBank accession number: KY635882) was selected as an outgroup following previous studies [40,41]. All the 23 cp genomes were annotated using the CpGAVAS2 pipeline [38], with *T. vernicifluum* 'Dahongpao' (GenBank accession number: MK550621) as the reference genome. Finally, nucleotide sequences of 77 common protein-coding genes were extracted, aligned, and concatenated using PhyloSuite 1.1.152 [42], resulting in an alignment of 67,432 bp in length.

Phylogenetic analyses were conducted using maximum likelihood (ML) and Bayesian Inference (BI) approaches for both un-partitioned sequence data and sequence data partitioned by genes. ModelFinder [43] was used to choose the optimal partitioning strategies and evolutionary models under the Bayesian Information Criterion (BIC). For the un-partitioned sequence data, TVM + F + R3 and GTR + F + I + G4 were selected as the best-fit substitution models for ML and BI analyses, respectively. For the sequence data partitioned by gene, the best-fit partition models were shown in Table S2. ML trees were reconstructed using IQ-tree 1.6.12 [44] with 10,000 ultrafast bootstrap (UFBS) replicates [45]. BI trees were built using MrBayes 3.2.6 [46]. Markov chain Monte Carlo (MCMC) runs were performed for 10 million generations, and trees were sampled every 1000 generations. The first 25% of the trees were discarded as burn-in to ensure that the chains were stationary. The remaining trees were used to generate a strict consensus tree and to calculate posterior probabilities for each node. All phylogenetic analyses mentioned above were conducted in Phylosuite 1.1.152 [42].

We used BEAST 2.6.7 [47] to estimate the divergence time among major cpDNA clades based on the concatenated sequences of 77 common protein-coding genes. The TVM + F + G4 model was selected as the best-fitting substitution model using ModelFinder [43] under the BIC. A combination of log-normal relaxed clock and Yule prior was used for node age estimation. Three calibration points were chosen according to previous phylogenetic studies of the genus *Toxicodendron* [48]. First, we used a secondary calibration point to set a normal prior with an offset of 74 million years ago (Ma), a mean of 0, and a sigma of 1.0 for the divergence between *Mangifera indica* and other members of the tribe Rhoeae (node I) [48]. Second, the reliable fossils of *Rhus* found in western North America in the middle Eocene [49] were used to set a log-normal prior with an offset of 44 Ma, a mean of 1.0, and a standard deviation of 0.85 for the stem age of *Rhus* (node II) [48]. Third, a leaf fossil of *Cotinus* found in North America in the early Oligocene/Late Eocene [50] was used to set a log-normal prior with an offset of 34 Ma, a mean of 1.0, and a standard deviation of 0.85 for the divergence between *Cotinus* and *Pistacia* (node III) [48]. Two independent MCMC runs were performed for 100 million generations and sampled every 10,000 generations. The generated log files were combined through LogCombiner 2.6.7 and then passed to Tracer 1.7.1 [51] for assessing convergence (effective sample size of all parameters > 200). TreeAnnotator 2.6.7 was used to construct a maximum clade credibility tree with a posterior probability limit of 0.5 and the first 25% of generations discarded as burn-in.

Table 1. Summary of the 22 complete chloroplast genomes of the tribe Rhoeae used by the phylogenetic analyses of this study. Those genomes belong to four genera, *Toxicodendron*, *Rhus*, *Cotinus*, and *Pistacia*. Newly generated sequences are marked by asterisks.

Species	Sources (Voucher Number)	GenBank acc. #	Length (bp)				GC (%)	Gene Number			
			Plastome	IRa/IRb	SSC	LSC		Full	PCG	tRNA	rRNA
T. vernicifluum	Qingzhou, Shandong, China (YTS1)	OQ168006 *	158,210	26,464	18,345	86,937	38.0	132	87	37	8
T. vernicifluum	Yantai, Shandong, China (KYS1)	OQ168008 *	158,209	26,464	18,344	86,937	38.0	132	87	37	8
T. vernicifluum	Huangshan, Anhui, China (AHH3)	OQ168009 *	158,223	26,464	18,345	86,950	38.0	132	87	37	8
T. vernicifluum	Jiaokou, Shanxi, China (JIK2)	OQ168007 *	159,593	26,512	19,070	87,499	37.9	132	87	37	8
T. vernicifluum	Leishan, Guizhou, China (LGS13)	OQ168010 *	159,565	26,513	19,071	87,468	38.0	132	87	37	8
T. vernicifluum	Xi'an, Shaanxi, China	MK419151	159,571	26,512	19,073	87,474	38.0	132	87	37	8
T. vernicifluum	Yangling, Shaanxi, China	MK550621	159,571	26,512	19,073	87,474	38.0	132	87	37	8
T. sylvestre	Lin'an, Zhejiang, China	MT211615	159,600	26,466	19,039	87,629	37.9	132	87	37	8
T. succedaneum	Chishui, Guizhou, China	MT211614	159,710	26,525	19,039	87,621	37.9	132	87	37	8
T. griffithii	Chenggan, Yunnan, China	MT269874	159,613	26,491	18,910	87,721	37.9	132	87	37	8
T. diversilobum	Washington Park, CA, USA	OP585546	159,543	26,526	18,796	87,695	38.0	132	87	37	8
R. chinensis	Shandong or Henan, China	MF351625	149,094	16,603	18,643	97,245	37.9	125	81	36	8
R. chinensis	Yanggu, Gangwon, South Korea	KX447140	149,011	16,742	18,646	96,881	37.8	125	81	36	8
R. hypoleuca	Unknown	MW238820	159,472	26,561	18,780	87,570	37.9	131	86	37	8
R. potaninii	Danfeng, Shaanxi, China	MT230556	159,620	26,476	18,947	87,721	37.9	132	87	37	8
R. punjabensis	Enshi, Hubei, China	MT230555	159,617	26,477	18,970	87,693	37.9	132	87	37	8
R. typhina	Mts. Lushan, Shandong, China	MT083895	160,204	26,549	19,318	87,788	37.8	132	87	37	8
R. wilsonii	Unknown	MW238821	159,814	26,528	18,842	87,916	37.8	132	87	37	8
C. coggygria	Mts. Jinyun, Chongqing, China	MT876478	158,843	26,830	18,063	87,120	38.0	131	85	38	8
P. weinmanniifolia	Unknown	MF630953	160,767	26,619	19,128	88,401	37.8	132	87	37	8
P. chinensis	Bazhong, Sichuan, China	MT157378	160,596	26,599	19,089	88,309	37.9	132	87	37	8
P. vera	Longnan, Gansu, China	MN551174	160,654	26,597	19,085	88,375	37.9	132	87	37	8

acc. #, accession number; GC, GC content; LSC, large single-copy; SSC, small single-copy; IR, inverted repeat; PCG, protein-coding gene.

2.4. Comparative Chloroplast Genome Analyses

The five newly sequenced and two previously published cp genomes of *T. vernicifluum* (GenBank accession number: MK419151 and MK550621) were aligned using MAFFT 7.3.13 [52] in the Phylosuite 1.1.152 platform [42]. The numbers of single nucleotide polymorphisms (SNPs) and insertion-deletion mutations (indels) in LSC, small single-copy (SSC) region, IRs, and protein-coding genes were counted by DnaSP 6.12.03 [53]. A TCS network was built with PopART 1.7 [54] based on the SNPs detected across the seven cp genomes.

To explore the highly variable regions across cp genomes of *T. vernicifluum* and its closely related species, shared genes, and intergenic regions were extracted by Phylosuite and aligned by MAFFT. The nucleotide diversity (π) values were calculated for 177 loci (114 genes and 63 intergenic spacers) across seven cp genomes of *T. vernicifluum*, for 176 loci (114 genes and 62 intergenic spacers) across 11 cp genomes of five *Toxicodendron* species, and for 167 loci (111 genes and 56 intergenic spacers) across 22 cp genomes of 15 species of the tribe Rhoeae (Table 1) using DnaSP 6.12.03 [53].

To investigate the genome variability of the seven cp genomes of *T. vernicifluum*, the mVISTA program was employed to plot the percentage of identity under the Shuffle-LAGAN mode, using the cp genome of *T. vernicifluum* YTS1 (GenBank accession number: OQ168006) as a reference [55]. Locally collinear blocks were identified by the Mauve module [56] in the Geneious 7.1.3 software [57] to detect the presence of large-scale evolutionary events such as rearrangements and inversions. The boundaries of LSC, SSC, and IR regions were visualized and compared among species using the IRscope software [58].

2.5. Repeat Sequence Identification

The REPuter online program [59] was used to identify large repetitive sequences, including forward, reverse, palindromic, and complementary repeats with the following parameters: minimum repeat size$\geq$30 bp, Hamming distance of 3, and maximum computed repeats of 50. Tandem Repeat Finder 4.09 [60] was used to identify tandem repeats, with the alignment weights for the match, mismatch, and indels set to 2, 7, and 7, respectively; matching probability (PM) and indel probability (PI) set to 80 and 10, respectively; minimum alignment score set to 50, and maximum period size set to 500. Simple sequence repeats (SSRs) were detected by the MISA-web tool [61,62] with the minimum repeat sizes for mono-, di-, tri-, tetra-, penta-, and hexanucleotides set to 10, 5, 4, 3, 3, and 3, respectively. The maximum sequence length between two SSRs for registration as a compound SSR was set to 100 bp.

2.6. Nuclear Ribosomal Internal Transcribed Spacer (ITS) Variation

We used the GetOrganelle 1.7.6.1 pipeline [33] to assemble the nuclear ribosomal DNA (rDNA) for the five newly sampled trees of *T. vernicifluum*. Assemblies were performed using the *k*-mer lengths of 35, 85, and 115 (i.e., -k 35, 85, 115). The maximum extension rounds (-R) were set to 10. The ITS sequences were extracted using the reference sequence of *T. succedaneum* (GenBank accession number: FJ945944). The obtained sequences were checked and aligned by BioEdit 7.2.5 [63]. ITS haplotypes were determined by DnaSP 6.12.03 [53]. A TCS network was constructed by PopART 1.7 [54].

3. Results and Discussion

3.1. Chloroplast Genome Assembly and Annotation

We assembled and annotated the complete cp genome sequences of five wild *T. vernicifluum* trees (Figure 1). After processing, a total of 60,743,870, 64,198,688, 64,056,786, 64,034,368, and 64,030,190 clean reads (150 bp in length) were obtained for samples YTS1, KYS1, AHH3, JIK2, and LGS13, respectively. The clean reads covered the entire assembled cp genome of the corresponding sample (100% coverage), representing an average depth of coverage of 3262.33×, 7762.28×, 8804.83×, 3986.53×, and 2658.80× for samples YTS1, KYS1, AHH3, JIK2, and LGS13, respectively. The newly generated plastomes were sub-

mitted to NCBI GenBank under accession numbers OQ168006–OQ168010. All five newly sequenced cp genomes encoded 132 genes, including 87 protein-coding genes, 37 tRNA genes, and eight rRNA genes (Figure 2). Among the 132 genes, 114 genes were unique, while 18 genes were duplicated, including seven protein-coding genes (*ndhB*, *rpl2*, *rpl23*, *rps12*, *rps7*, *ycf2*, and *ycf15*), seven tRNA genes (*trnA-UGC*, *trnI-CAU*, *trnI-GAU*, *trnL-CAA*, *trnN-GUU*, *trnR-ACG*, and *trnV-GAC*), and four rRNA genes (*rrn16*, *rrn23*, *rrn4.5*, and *rrn5*). These results were consistent with those of two previously reported accessions of *T. vernicifluum* (GenBank accession number: MK419151 and MK550621) [64,65] and with those of the other four species of *Toxicodendron* [21–23,66] (Table 1), suggesting that the cp genomes of *Toxicodendron* are highly conserved in gene content and order [67].

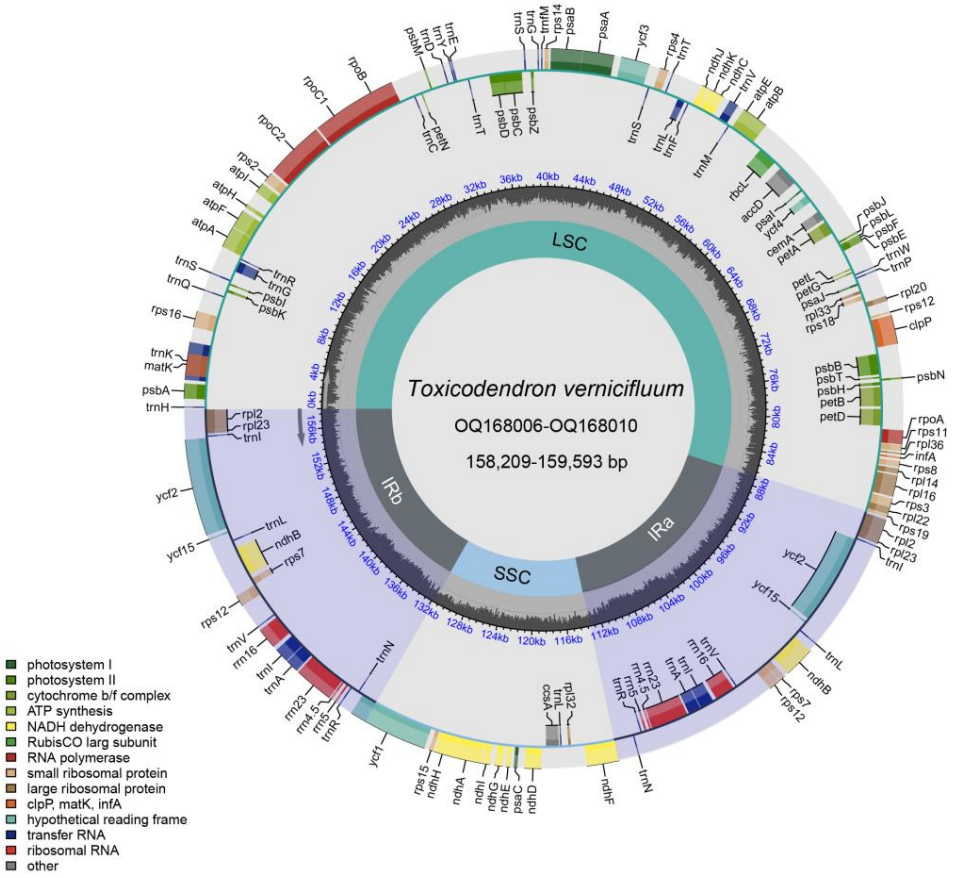

Figure 2. Gene circle map for the five newly sequenced chloroplast genomes of *Toxicodendron vernicifluum*. The genes were color-coded according to different functional groups. Genes on the inside and outside of the large circle are transcribed clockwise and counterclockwise, respectively. The darker gray columns in the inner circle correspond to the GC content. The circle map was generated by the CPGView online tool (http://www.1kmpg.cn/cpgview) (accessed on 1 January 2023).

3.2. Phylogenetic Analyses Based on Chloroplast Genome Sequences

We reconstructed the phylogenetic relationships of 22 accessions of the tribe Rhoeae (Table 1) and one outgroup based on 77 common protein-coding genes of cp genomes. The ML and BI analyses yielded similar tree topologies for both un-partitioned sequence data and sequence data partitioned by gene (Figures 3, S1 and S2). Our results supported the monophyly of *T. vernicifluum* [un-partitioned data: posterior probability (PP) = 1, bootstrap support value (BS) = 100; partitioned data: PP = 1, BS = 100]. These findings were consistent with previous studies showing that *T. vernicifluum* did not share any cpDNA haplotypes with closely related species such as *T. griffithii*, *T. radicans*, *T. succedaneum*, *T. sylvestre*, and *T. trichocarpum* [1,7], indicating that cpDNA markers could be effective in the delimitation of *T. vernicifluum* and its relatives. However, given that introgression and shared ancestral

polymorphism may result in interspecific cpDNA sharing, it is necessary to include more samples of closely related species with overlapping distributions in future work to better understand the cpDNA phylogeny of *T. vernicifluum* and its congeners [17–19].

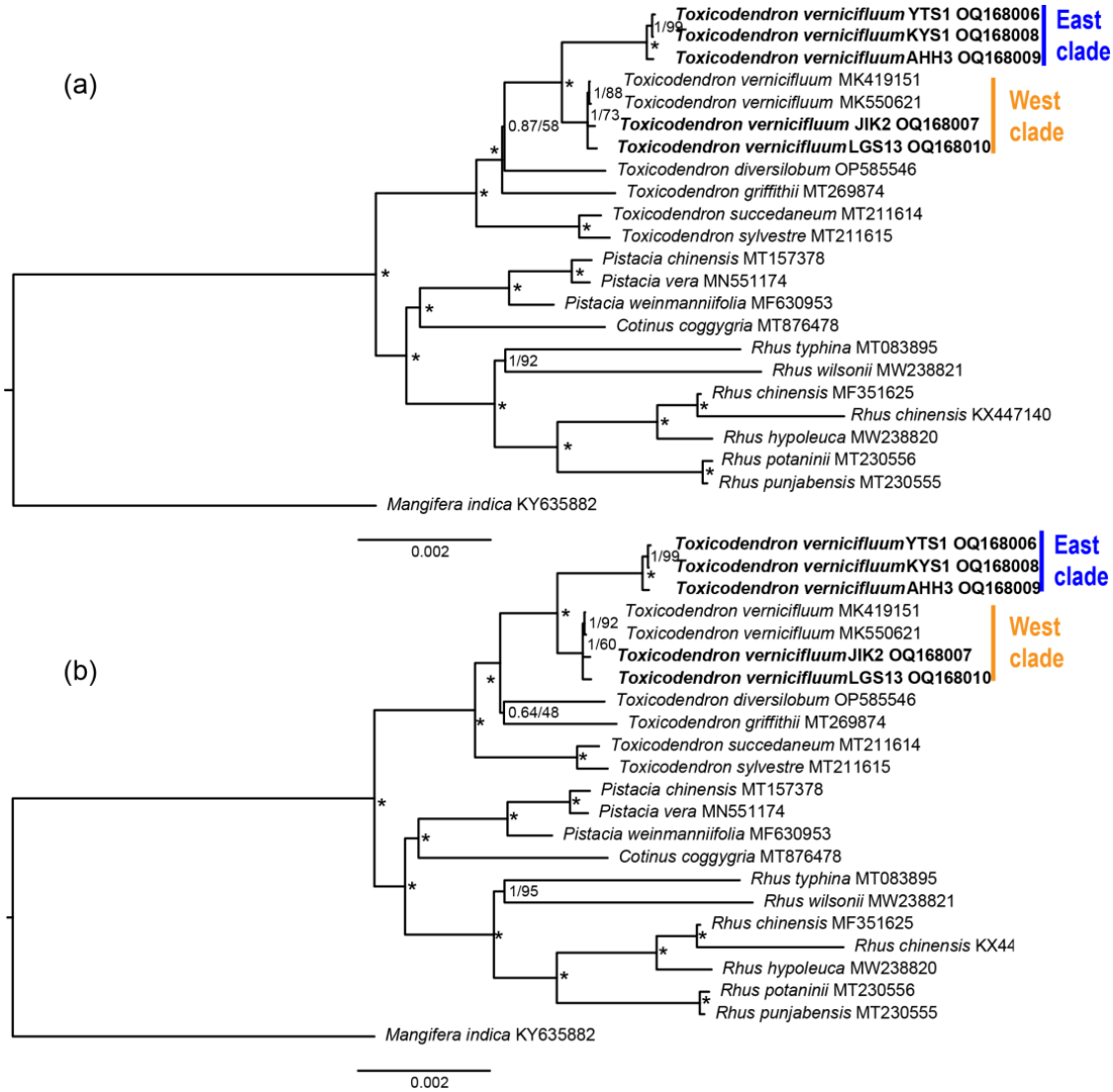

Figure 3. Phylogenetic trees inferred from maximum likelihood (ML) and Bayesian Inference (BI) approaches for (**a**) sequence data partitioned by genes and (**b**) un-partitioned sequence data. Numbers near the nodes are Bayesian posterior probabilities (PP, left of the slashes) and ML bootstrap support values (BS, right of the slashes). Nodes with PP of 1 and BS of 100 are marked by asterisks. Newly generated sequences in this study are indicated in bold.

Complete cp genomes contain more phylogenetic information that would be useful for evaluating intraspecific genetic relationships [68]. Our results showed the four *T. vernicifluum* individuals from western China (JIK2, LGS13, MK419151, and MK550621) formed a monophyletic group (un-partitioned data: PP = 1, BS = 100; partitioned data: PP = 1, BS = 100) sister to the cluster containing the three individuals from eastern China (YTS1, KYS1, and AHH3) (un-partitioned data: PP = 1, BS = 100; partitioned data: PP = 1, BS = 100). These results indicated that the cp genomes of *T. vernicifluum* split into two main clades: western China and eastern China lineages (Figure 3), supporting the conclusions of recent phylogeographic studies that an east-west phylogeographic split occurred in *T. vernicifluum* [1,7].

In western China, we found that the individual from southwestern China (LGS13, from the Guizhou Province) represented the basal branch, while the two individuals from northwestern China (MK419151 and MK550621, from the Shaanxi Province) formed a subclade (un-partitioned data: PP = 1, BS = 92; partitioned data: PP = 1, BS = 88) sister to that from northern China (JIK2, from the Shanxi Province). These results suggested that the *T. vernicifluum* trees may have undergone north-south divergence among the mountainous areas in western China. However, such patterns were not recovered by previous studies using only two cpDNA fragments [1,7].

In eastern China, we found that the two individuals from northeastern China (YTS1 and KYS1, from the Shandong Province) formed a subclade (un-partitioned data: PP = 1, BS = 99; partitioned data: PP = 1, BS = 99) sister to the individual from southeastern China (AHH3, from the Anhui Province). These findings supported that the *T. vernicifluum* trees may have also undergone north-south divergence in eastern China, congruent with previous results that two dominant chloroplast haplotypes were detected in the *T. vernicifluum* populations of northeastern and southeastern China [1,7].

Our results supported the monophyly of the genus *Toxicodendron* (un-partitioned data: PP = 1, BS = 100; partitioned data: PP = 1, BS = 100), which was found to be sister to the clade containing the remaining genera *Rhus*, *Cotinus*, and *Pistacia*. The topology of the tribe Rhoeae reported here was consistent with previous results obtained by nuclear and cpDNA fragments [48] or complete cp genome sequences [28]. However, the phylogenetic relationships of *Toxicodendron* species were not fully resolved (Figure 3). Using both nuclear and chloroplast DNA sequence data, previous studies have shown that *T. vernicifluum* was more closely related to *T. sylvestre* and *T. succedaneum* than to *T. griffithii* and *T. diversilobum*, implying the possibility of cyto-nuclear discordance in the phylogeny of *Toxicodendron* [69].

3.3. Divergence Time Estimation

The BEAST analyses grouped the seven *T. vernicifluum* individuals into eastern and western clades (Figure 4), which was consistent with the results of ML/BI analyses (Figure 3). The divergence time between the two clades was estimated to be 11.30 Ma (95% HPD: 4.18–22.47 Ma), suggesting that the two lineages may have diverged during the Late Miocene. This timing is comparable with the initial intraspecific divergence time of *Kerria japonica* (7.78 Ma; during the Late Miocene), a woody plant also presenting east-west phylogeographical breaks along the boundaries of the three-step landforms of China [70]. These findings implied that the geological and climatic events during the Late Miocene (e.g., Asian monsoon intensifications) may have been responsible for the onset of intraspecific diversification of *T. vernicifluum* [70]. The crown ages of the eastern and western clades of *T. vernicifluum* were estimated to be 1.80 Ma (95% HPD: 0.36–5.09 Ma) and 1.68 Ma (95% HPD: 0.39–4.51 Ma), respectively, suggesting that the Pleistocene climate fluctuations may have further driven the intraspecific cpDNA differentiation of *T. vernicifluum*.

3.4. Chloroplast Genome Comparison among the Accessions of T. vernicifluum, Toxicodendron, and the Tribe Rhoeae

All seven cp genomes of *T. vernicifluum* possessed a typical quadripartite structure, comprising one LSC region and one SSC region that were separated by two IRs (Figure 2). The seven cp genomes had similar GC contents (37.9–38.0%) but varied in genome length (Table 1). Compared with the three *T. vernicifluum* individuals from eastern China (average cp genome length: 158,214 bp), the four individuals from western China had larger cp genome length (average cp genome length: 159,575 bp) (Table 1). This was mainly attributed to that the SSC and LSC regions of the western China accessions were on average 727 and 537 bp longer than those of the eastern China accessions, respectively. Furthermore, the two IRs of the western China accessions were on average 96 bp longer than those of the eastern China accessions.

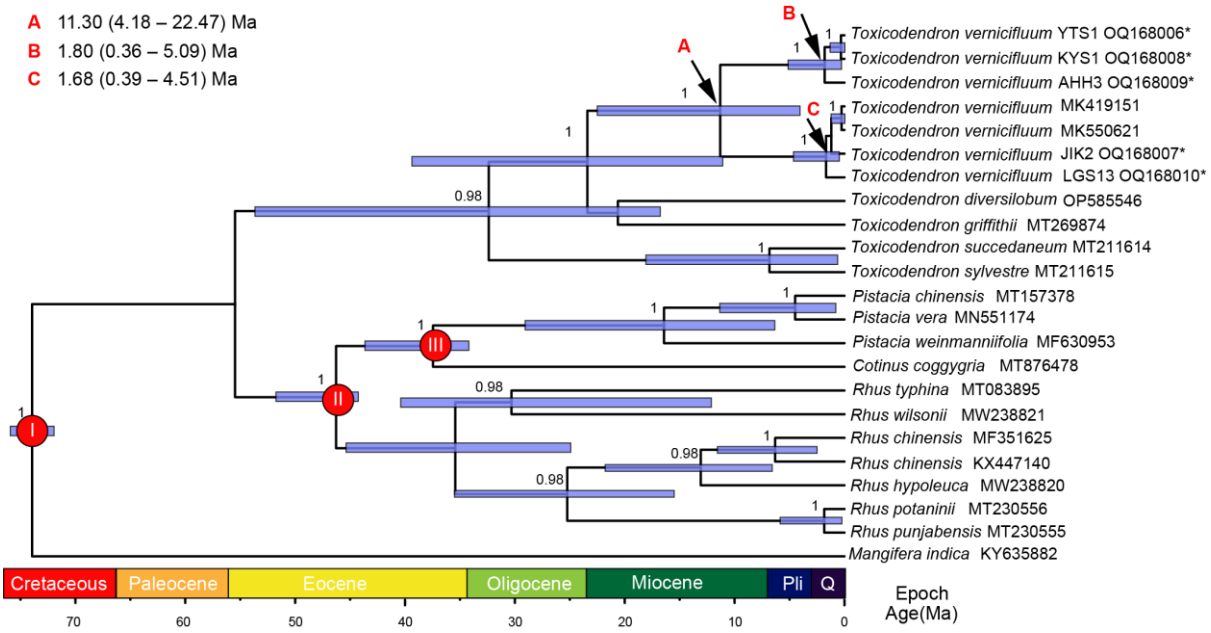

Figure 4. BEAST-derived chronogram for 22 individuals of the tribe Rhoeae, with *Mangifera indica* as an outgroup. Blue bars indicate the 95% highest posterior density (HPD) credibility intervals for node ages (million years ago, Ma). Posterior probabilities (>0.9) are labeled above nodes. Node I, II, and III are calibration points. Geological time abbreviations: Pli, Pliocene; Q, Quaternary.

The aligned cp genome sequences of the seven *T. vernicifluum* individuals were 159,932 bp in length. A total of 466 SNPs (0.29%) and 141 indels were detected (Table 2). The majority of the SNPs and indels were present in the LSC regions (331/109), followed by the SSC (111/20) and IR regions (24/12). The TCS network grouped the seven *T. vernicifluum* individuals into two clades: the eastern and western clades (Figure 5a). Those two clades were separated by 383 SNPs, indicating that most SNPs detected among the seven cp genomes existed between the eastern and western groups. Furthermore, SNPs and indels detected among the four *T. vernicifluum* individuals from western China were more than those found among the individuals from eastern China. No variations were found in the IR regions of the eastern China individuals.

Table 2. The numbers and distributions of single nucleotide polymorphisms (SNPs) and insertion-deletion mutations (indels) detected among the seven chloroplast genomes of *Toxicodendron vernicifluum*.

Index	Eastern Group	Western Group	All Samples
Number of samples	3	4	7
Aligned length (bp)	158,244	159,608	159,932
Total numbers of SNPs and indels	18/20	68/17	466/141
Numbers of SNPs and indels in LSC	11/17	50/13	331/109
Numbers of SNPs and indels in SSC	7/3	16/2	111/20
Numbers of SNPs and indels in IRs	0/0	2/2	24/12
Numbers of SNPs and indels in PCGs	14/0	19/0	150/39

LSC, large single-copy; SSC, small single-copy; IR, inverted repeat; PCG, protein-coding gene.

Chloroplast genomes of plants can provide highly variable regions that can be used as potential molecular markers for species identification and intra-/interspecific evolutionary studies [71,72]. We calculated the nucleotide diversity (π) values for common genes and intergenic regions across cp genomes to determine the hotspots of divergence at different taxonomic levels. The π values among the cp genomes of seven accessions of *T. vernicifluum*, 11 accessions of *Toxicodendron*, and 22 accessions of the tribe Rhoeae (Table 1) ranged from 0 to 0.126, from 0 to 0.129, from 0 to 0.036, respectively. Generally, intergenic spacers (average

π = 0.006, 0.009, 0.014 at the three taxonomic levels mentioned above) were found to be more variable than genes (average π = 0.001, 0.002, 0.005 at the three taxonomic levels mentioned above). Among the seven *T. vernicifluum* accessions, two gene regions (*rpl32* and *rps19*) and six intergenic regions (*trnF-ndhJ*, *rpl32-trnL*, *ccsA-ndhD*, *trnH-psbA*, *psbC-trnS*, and *trnL-trnF*) were identified as divergence hotspots based on the cutoff value of $\pi \geq 0.007$ (Figure 6). Among the 11 accessions of *Toxicodendron*, one gene region (rps19) and eight intergenic regions (*trnF-ndhJ*, *trnH-psbA*, *petD-rpoA*, *ccsA-ndhD*, *rpl32-trnL*, *atpF-atpH*, *trnL-trnF*, and *psbC-trnS*) were identified as divergence hotspots based on the cutoff value of $\pi \geq 0.013$ (Figure S3). Among the 22 accessions of the tribe Rhoeae, one gene region (psbM) and ten intergenic regions (*ccsA-ndhD*, *trnS-psbZ*, *petD-rpoA*, *ycf4-cemA*, *ndhG-ndhI*, *matK-rps16*, *trnD-trnY*, *trnL-trnF*, *ndhE-ndhG*, and *trnS-trnG*) were identified as divergence hotspots based on the cutoff value of $\pi \geq 0.002$ (Figure S4). Overall, the regions *trnF-ndhJ*, *rpl32-trnL*, *trnH-psbA*, *psbC-trnS*, and *rps19* were suitable for both phylogeographic studies of *T. vernicifluum* and phylogenetic studies of *Toxicodendron*, while the regions *ccsA-ndhD* and *trnL-trnF* were useful for evolutionary studies at all the three taxonomic levels. The mutational hotspots identified here also overlapped with those previously reported for six Anacardiaceae species [64], including *trnH-psbA*, *atpF-atpH*, *ccsA-ndhD*, *petD-rpoA*, and *trnL-trnF*. These hotspot regions could be utilized as potential molecular markers for reconstructing the phylogeny of *Toxicodendron* species and their relatives.

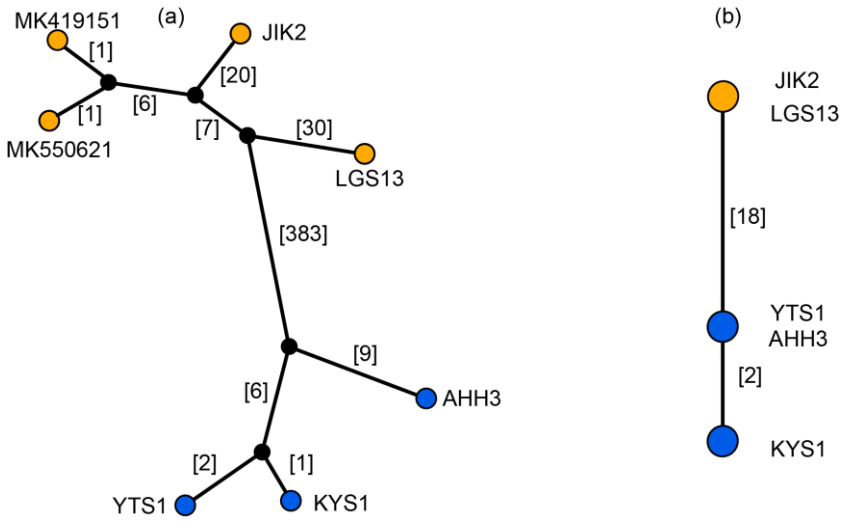

Figure 5. TCS network of the seven chloroplast (cp) genome sequences (**a**) and three nuclear ribosomal internal transcribed spacer (ITS) haplotypes (**b**) of *Toxicodendron vernicifluum*. The two networks were constructed by PopART 1.7. Numbers in brackets indicate the number of mutations between haplotypes. Samples from eastern and western China are marked in blue and orange, respectively. Note that two previously published cp genomes of *T. vernicifluum* (GenBank accession number: MK419151 and MK550621) are included in panel (**a**).

The hotspots of divergence identified above were also validated by the mVISTA analysis. We used the mVISTA program to plot the percentage of identity of seven *T. vernicifluum* individuals to investigate sequence divergence with YTS1 as a reference. As expected, a high similarity was found among the accessions of *T. vernicifluum*, with the IRs found to be more conserved than the LSC/SSC regions (Figure 7) [73,74]. The non-coding regions were significantly more variable than the coding regions. Consistent with the results of π value calculations, a high level of divergence was found for regions such as *ccsA-ndhD*, *trnH-psbA*, *rpl32-trnL*, and *trnF-ndhJ* between the individuals from eastern and western China. We also used the Mauve module to perform the synteny analysis. One local collinear block was detected and no rearrangement events and inversions were identified among the accessions of *T. vernicifluum* (Figure S5), *Toxicodendron* (Figure S6), and the tribe Rhoeae (Figure S7).

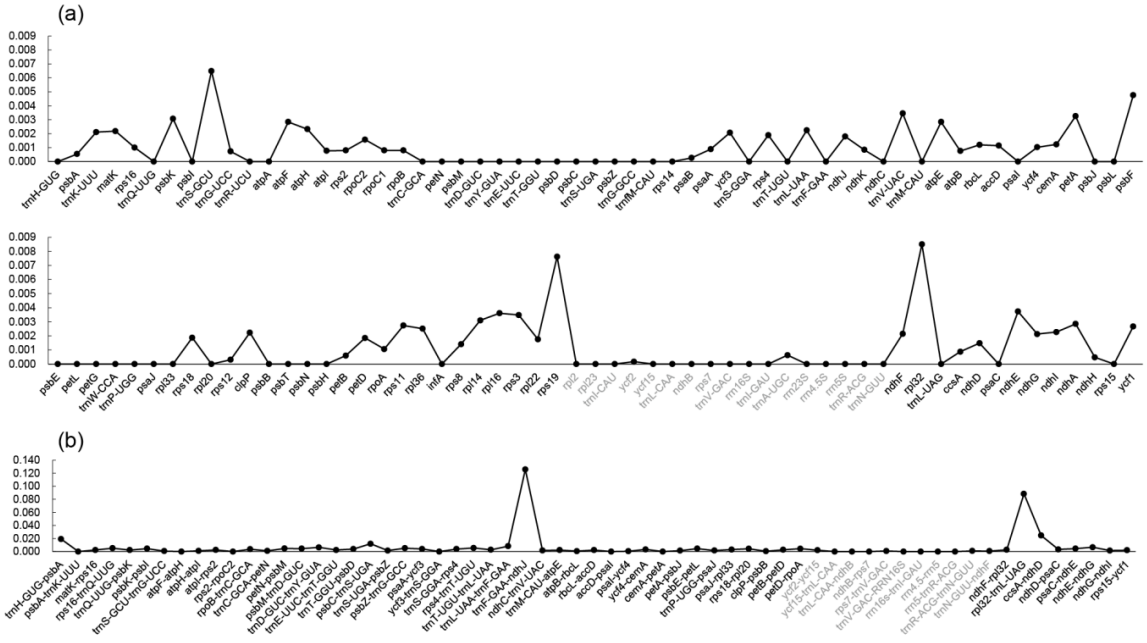

Figure 6. Nucleotide diversity (π) values estimated for 114 genes (**a**) and 63 intergenic regions (**b**) across the seven chloroplast genomes of *Toxicodendron vernicifluum* (GenBank accession number: OQ168006–OQ168010, MK419151, MK550621). Loci in the inverted repeats (IRs) are marked in gray. Note that the scales of the y-axis differ between (**a**,**b**).

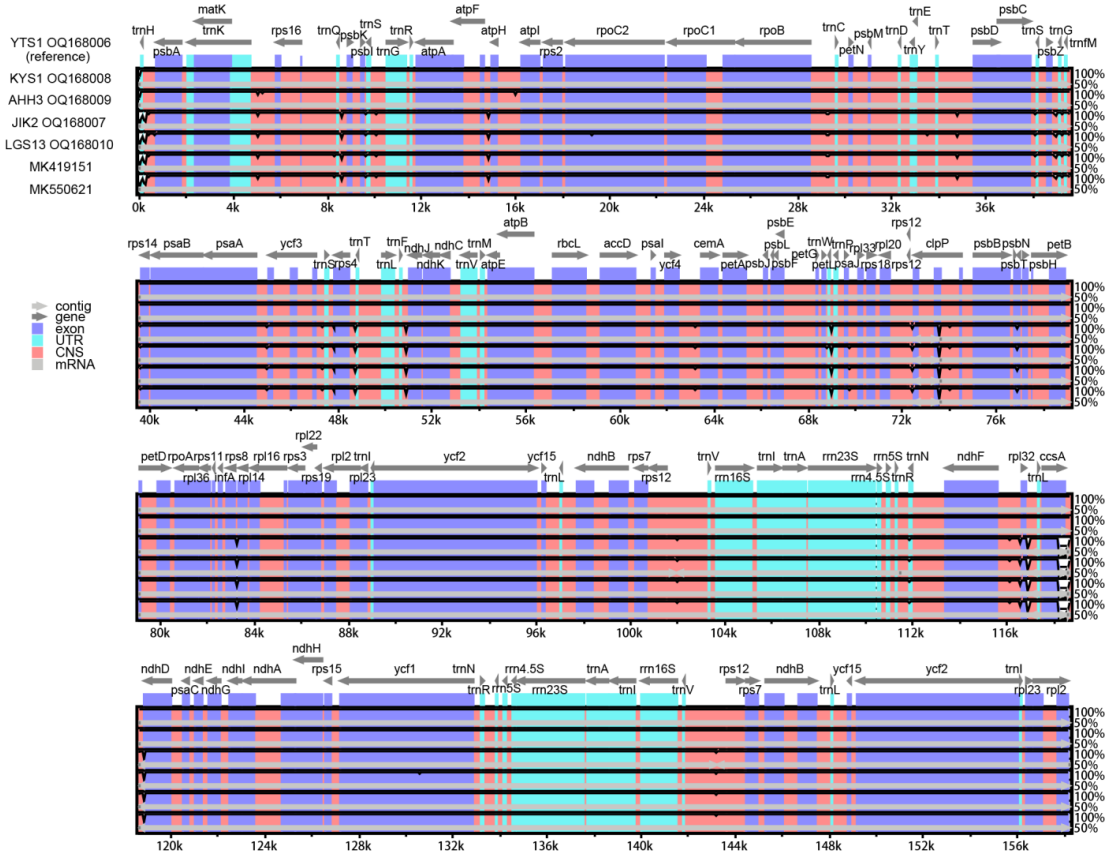

Figure 7. Sequence alignment of seven *Toxicodendron vernicifluum* chloroplast genomes using mVISTA with *T. vernicifluum* YTS1 as a reference. The vertical scale indicates the percent identity, ranging from 50% to 100%. The horizontal axis shows the location within the plastomes. Genome regions are color-coded as exon, intron, and untranslated regions (UTRs).

3.5. Expansion and Contraction of the IR Regions

The IR-SC border positions of the cp genomes of *T. vernicifluum* and the other four *Toxicodendron* species were highly conserved (Figure 8) [75]. The LSC/IRb junction was found between the genes *rps19* and *rpl2*. The IRb/SSC junction was found within the gene *ndhF*. The SSC/IRa junction was found within the gene *ycf1*. The IRa/LSC junction was found between the genes *rpl2* and *trnH*. Minor shifts of the IRa/LSC boundary were detected among *Toxicodendron* accessions. Specifically, the *trnH* gene was found to be 64 bp and 47 bp away from the IRa/LSC boundary for the *T. vernicifluum* individuals from eastern China and western China, respectively (Figure 8). Furthermore, the *trnH* gene was found to be 30–54 bp away from the IRa/LSC boundary for the other four *Toxicodendron* species (Figure 8).

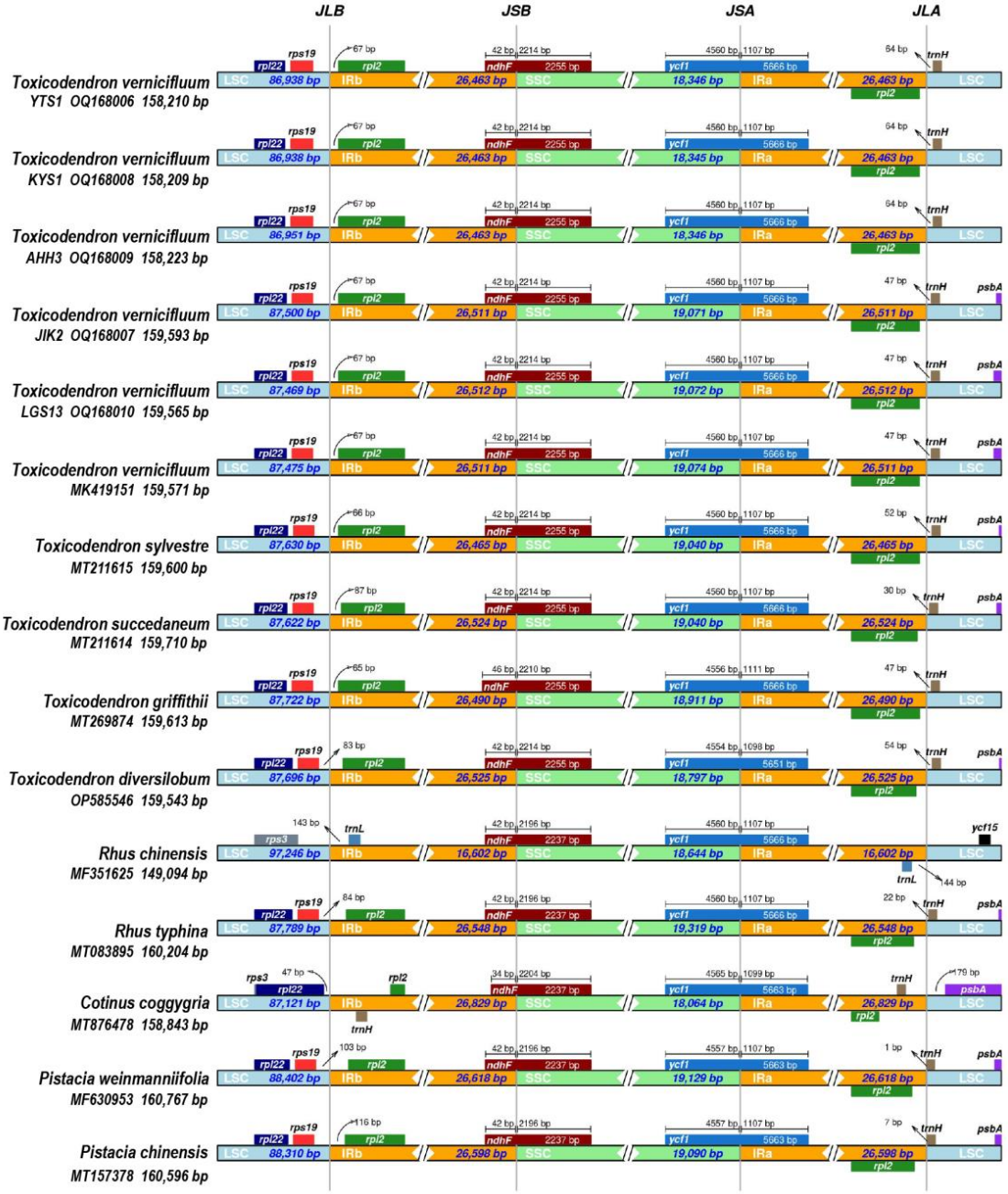

Figure 8. Comparison of inverted repeat (IR)-single-copy (SC) border positions among the chloroplast genomes of 15 accessions of the tribe Rhoeae. The sequence of *T. vernicifluum* MK550621 was not used because it differed from that of MK419151 by only two single nucleotide variants.

Compared to the species from other genera in the tribe Rhoeae, visible differences were detected regarding the lengths of IR regions (Table 1) and the SC/IR borders (Figure 8). Among those, *Rhus chinensis* presented the most significant difference from other species: its LSC/IRb border was located between the genes *rps3* and *trnL*, while its IRa/LSC border was located between the genes *trnL* and *ycf15*. This shift was mainly attributed to the loss of a long fragment (~9800 bp in length) in the IR regions of *R. chinensis*, which contains genes such as *rpl2*, *rpl23*, *trnI-CAU*, and *ycf2* [29,64]. In addition, compared to other species, *rps19* was lost at the border of IRb/LSC and *trnH* was shifted from LSC to IRa in *Cotinus coggygria*.

3.6. Repeat Sequence Identification

For the *T. vernicifluum* individuals from eastern China, 68–69 SSRs were detected for each accession, including 43–44 mononucleotide SSRs, five dinucleotide SSRs, six trinucleotide SSRs, five tetranucleotide SSRs, one pentanucleotide SSR, and 7–9 compound SSRs (Table S3). For the *T. vernicifluum* individuals from western China, 66 SSRs were detected for each accession, including 45 mononucleotide SSRs, five dinucleotide SSRs, five trinucleotide SSRs, five tetranucleotide SSRs, one pentanucleotide SSR, and five compound SSRs. For the other four species of *Toxicodendron*, 71–82 SSRs were detected for each accession, including 46–56 mononucleotide SSRs, 4–5 dinucleotide SSRs, 4–5 trinucleotide SSRs, 4–5 tetranucleotide SSRs, one pentanucleotide SSR, and 10–13 compound SSRs. Overall, the two groups of *T. vernicifluum* had a similar number of SSRs, while the other four *Toxicodendron* species had more SSRs mainly because of their higher numbers of mononucleotide SSRs and compound SSRs.

Long-dispersed repeat sequences have been reported to play critical roles in genomic rearrangements and sequence variations of plastomes [76]. A total of 49 long dispersed repeats were detected for each accession of *T. vernicifluum* and the other four *Toxicodendron* species, with a length ranging from 30 to 78 bp (Table S4). Specifically, 20–21 forward repeats and 28 palindromic repeats were detected for each *T. vernicifluum* accession from eastern China; 22 forward repeats and 26 palindromic repeats were detected for each *T. vernicifluum* accession from western China; 21–22 forward repeats and 27–28 palindromic repeats were detected for each accession of the other four *Toxicodendron* species. Reverse repeats were only detected in the LSC region of *T. vernicifluum* accessions from western China, while complementary repeats were only detected in the IRs of *T. vernicifluum* accessions from eastern China. Furthermore, 46–47, 47, and 40–50 tandem repeats were detected for *T. vernicifluum* accession from eastern China, *T. vernicifluum* accession from western China, and accessions of the other four *Toxicodendron* species, respectively (Table S4).

3.7. Nuclear Ribosomal Internal Transcribed Spacer (ITS) Variation

A total of three ITS haplotypes were found for the five individuals of *T. vernicifluum*. The TCS network grouped them into eastern and western clades that were separated by 18 mutational steps (Figure 5b). Specifically, the two individuals from western China (JIK2 and LGS13) shared one ITS haplotype, while the other two individuals from eastern China (YTS1 and AHH3) shared another ITS haplotype that differed from the ITS haplotype of KYS1 by two mutational steps. The east-west divergence pattern recovered by ITS variation was consistent with the findings based on whole cp genome sequence variation (Figure 5a).

4. Conclusions

In this study, we sequenced five cp genomes of *T. vernicifluum* representing the wild individuals from eastern and western China. Our phylogenetic analyses based on protein-coding genes supported that the species split into two main clades: western China and eastern China lineages. Generally, chloroplast genomes of *T. vernicifluum* individuals from eastern and western China were highly conserved in terms of structure and gene content. However, obvious differences were still detected between them. The genome lengths of western China individuals were on average 1361 bp larger than that of eastern China individuals. The LSC, SSC, and two IR regions of western China individuals were also

found to be longer than those of eastern China individuals. Most of the SNPs and indels detected among the *T. vernicifluum* accessions occurred between the eastern and western lineages. Furthermore, complementary repeat sequences were only found in the individuals of eastern China while reverse repeats were only detected in the individuals from western China. Numerous mutational hotspots (e.g., *trnF-ndhJ*, *rpl32-trnL*, *ccsA-ndhD*, *trnH-psbA*, *psbC-trnS*, *trnL-trnF*, *rpl32*, and *rps19*) were also identified which can be used as potential molecular markers in phylogenetic analysis. The genomic resources presented in this study will be useful for further studies on evolutionary patterns and resource protection of *T. vernicifluum.*

Supplementary Materials: The following supporting information can be downloaded at: https://www.mdpi.com/article/10.3390/f14040818/s1, Figure S1: Phylogenetic trees inferred by the maximum likelihood (ML) approach for (a) sequence data partitioned by genes and (b) un-partitioned sequence data; Figure S2: Phylogenetic trees inferred by the Bayesian Inference (BI) approach for (a) sequence data partitioned by genes and (b) un-partitioned sequence data; Figure S3: Nucleotide diversity (π) among the complete chloroplast genome sequences of 11 accessions of *Toxicodendron*; Figure S4: Nucleotide diversity (π) among the complete chloroplast genome sequences of 22 accessions of the tribe Rhoeae; Figure S5: Gene map and MAUVE alignment of six chloroplast genomes of *Toxicodendron vernicifluum*; Figure S6: Gene map and MAUVE alignment of five chloroplast genomes of *Toxicodendron*; Figure S7: Gene map and MAUVE alignment of six chloroplast genomes of the tribe Rhoeae; Table S1: Geographic information of the five newly sequenced *Toxicodendron vernicifluum* samples in this study; Table S2: Optimal partitioning strategies and evolutionary models selected by ModelFinder using the Bayesian Information Criterion (BIC); Table S3: Numbers of simple sequence repeats (SSRs) of the 11 *Toxicodendron* plastomes; Table S4: Numbers of long dispersed repeats and tandem repeats in the 11 *Toxicodendron* plastomes.

Author Contributions: L.W., Y.F. and F.Z. conceived and designed this research. L.W., Y.L., Y.P. and F.Z. collected samples. L.W. performed experiments. L.W., N.H., Y.L. and X.Z. analyzed the data. L.W. wrote the original draft. X.Z., Y.L., Y.P. and Y.F. reviewed the draft. Y.F. and F.Z. supervised the project. All authors have read and agreed to the published version of the manuscript.

Funding: This research was supported by the Shaanxi Innovation Capability Support Plan "Fenxi Inspection and Testing Shared Experimental Base" (2023-CX-PT-08), Research and Development Program of Key Technologies for Conservation and Restoration of Two Wild Plant Species with Extremely Small Populations in the Mingxi County (22100210), the Natural Science Foundation from Education Commission of Anhui Province (2022AH050369), the National Natural Science Foundation of China (32201375), the China Postdoctoral Science Foundation (2020M681629), the Jiangsu Postdoctoral Research Foundation (2021K038A), and the Priority Academic Program Development of Jiangsu Higher Education Institutions (PAPD). L. W. was supported by the China Scholarship Council (202008320479).

Institutional Review Board Statement: Not applicable.

Informed Consent Statement: Not applicable.

Data Availability Statement: The newly generated chloroplast genome sequences of *Toxicodendron vernicifluum* were submitted to NCBI under GenBank accession numbers OQ168006–OQ168010. The nuclear ribosomal internal transcribed spacer (ITS) data were available from Zenodo: https://doi.org/10.5281/zenodo.7792326.

Acknowledgments: We thank numerous Chinese foresters and natural resource managers for their help in the sample collection.

Conflicts of Interest: The authors declare no conflict of interest.

References

1. Suzuki, M.; Noshiro, S.; Tanaka, T. Origin of urushi (*Toxicodendron vernicifluum*) in the neolithic Jomon period of Japan. *Bull. Nat. Mus. Jpn. Hist.* **2014**, *187*, 49–70.
2. Zhao, M.; Liu, C.; Zheng, G. Comparative studies of bark structure, lacquer yield and urushiol content of cultivated *Toxicodendron vernicifluum* varieties. *New. Zeal. J. Bot.* **2013**, *51*, 13. [CrossRef]

3. Hong, D.H.; Han, S.B.; Lee, C.W.; Park, S.H.; Jeon, Y.J.; Kim, M.J.; Kwak, S.S.; Kim, H.M. Cytotoxicity of urushiols isolated from sap of Korean lacquer tree (*Rhus vernicifera* Stokes). *Arch. Pharm. Res.* **1999**, *22*, 638–641. [CrossRef] [PubMed]
4. Cho, N.; Choi, J.H.; Yang, H. Neuroprotective and anti-inflammatory effects of flavonoids isolated from *Rhus verniciflua* in neuronal HT22 and microglial BV2 cell lines. *Food Chem. Toxicol.* **2012**, *50*, 1940–1945. [CrossRef]
5. Suzuki, M.; Yonekura, K.; Noshiro, S. Distribution and habitat of *Toxicodendron vernicifluum* (Stokes) F. A. Barkl. (*Anacardiaceae*) in China. *Jpn. J. Histor. Bot.* **2007**, *15*, 58–62.
6. Noshiro, S.; Suzuki, M. *Rhus verniciflua* Stokes grew in Japan since the Early Jomon Period. *Jpn. J. Histor. Bot.* **2004**, *12*, 3–11.
7. Wang, L.; Li, Y.; Noshiro, S.; Suzuki, M.; Arai, T.; Kobayashi, K.; Xie, L.; Zhang, M.Y.; He, N.; Fang, Y.M.; et al. Stepped geomorphology shaped the phylogeographic structure of a widespread tree species (*Toxicodendron vernicifluum*, *Anacardiaceae*) in East Asia. *Front. Plant Sci.* **2022**, *13*, 920054. [CrossRef]
8. Moore, M.J.; Soltis, P.S.; Bell, C.D.; Burleigh, J.G.; Soltis, D.E. Phylogenetic analysis of 83 plastid genes further resolves the early diversification of eudicots. *Proc. Natl. Acad. Sci. USA* **2010**, *107*, 4623–4628. [CrossRef]
9. Liu, L.; Wang, Y.; He, P.; Li, P.; Lee, J.; Soltis, D.E. Chloroplast genome analyses and genomic resource development for epilithic sister genera *Oresitrophe* and *Mukdenia* (*Saxifragaceae*), using genome skimming data. *BMC Genom.* **2018**, *19*, 235. [CrossRef]
10. Daniell, H.; Lin, C.S.; Yu, M.; Chang, W.J. Chloroplast genomes: Diversity, evolution, and applications in genetic engineering. *Genome Biol.* **2016**, *17*, 134. [CrossRef]
11. Meyer, C.P.; Paulay, G. DNA barcoding: Error rates based on comprehensive sampling. *PLoS Biol.* **2005**, *3*, e422. [CrossRef] [PubMed]
12. Birky, C.W. Uniparental inheritance of mitochondrial and chloroplast genes: Mechanisms and evolution. *Proc. Natl. Acad. Sci. USA* **1995**, *92*, 11331–11338. [CrossRef] [PubMed]
13. Dong, W.; Xu, C.; Cheng, T.; Lin, K.; Zhou, S. Sequencing angiosperm plastid genomes made easy: A complete set of universal primers and a case study on the phylogeny of Saxifragales. *Genome Biol. Evol.* **2013**, *5*, 989–997. [CrossRef] [PubMed]
14. Alkan, C.; Sajjadian, S.; Eichler, E.E. Limitations of next-generation genome sequence assembly. *Nat. Methods* **2011**, *8*, 61–65. [CrossRef] [PubMed]
15. Song, H.; Liu, F.; Li, Z.; Xu, Q.; Chen, Y.; Yu, Z.; Chen, N.S. Development of a high-resolution molecular marker for tracking *Phaeocystis globosa* genetic diversity through comparative analysis of chloroplast genomes. *Harmful Algae* **2020**, *99*, 101911. [CrossRef] [PubMed]
16. Xu, K.; Lin, C.; Lee, S.Y.; Mao, L.; Meng, K. Comparative analysis of complete *Ilex* (*Aquifoliaceae*) chloroplast genomes: Insights into evolutionary dynamics and phylogenetic relationships. *BMC Genom.* **2022**, *23*, 203. [CrossRef]
17. Huang, D.; Hefer, C.; Kolosova, N.; Douglas, C.; Cronk, Q. Whole plastome sequencing reveals deep plastid divergence and cytonuclear discordance between closely related balsam poplars, *Populus balsamifera* and *P. trichocarpa* (*Salicaceae*). *New Phytol.* **2014**, *204*, 693–703. [CrossRef]
18. Li, Y.; Wang, L.; Zhang, X.; Kang, H.; Liu, C.; Mao, L.; Fang, Y. Extensive sharing of chloroplast haplotypes among East Asian Cerris oaks: The imprints of shared ancestral polymorphism and introgression. *Ecol. Evol.* **2022**, *12*, e9142. [CrossRef]
19. Fahey, P.S.; Fowler, R.M.; Udovicic, F.; Cantrill, D.J.; Bayly, M.J. Use of plastid genome sequences in phylogeographic studies of tree species can be misleading without comprehensive sampling of co-occurring, related species. *Tree Genet. Genomes* **2021**, *17*, 43. [CrossRef]
20. Min, T.; Barfod, A. Anacardiaceae. In *Flora of China*; Wu, Z., Raven, P.H., Hong, D., Eds.; Science Press: Beijing, China; Missouri Botanical Garden Press: St. Louis, MA, USA, 2008; Volume 11, pp. 335–357.
21. Wang, L.; He, N.; Li, Y.; Fang, Y.; Zhang, F. The complete chloroplast genome sequence of *Toxicodendron succedaneum* (*Anacardiaceae*). *Mitochondrial DNA Part B* **2020**, *5*, 1956–1957. [CrossRef]
22. Li, Y.; Tang, Y.; Wu, T. The complete chloroplast genome of *Toxicodendron griffithii*. *Mitochondrial DNA Part B* **2020**, *5*, 2211–2212. [CrossRef]
23. Weisberg, A.J.; Kim, G.; Westwood, J.H.; Jelesko, J.G. Sequencing and de novo assembly of the *Toxicodendron radicans* (*poison ivy*) transcriptome. *Genes* **2017**, *8*, 317. [CrossRef] [PubMed]
24. Xu, L.; Zhou, N.; Zhao, S.; Li, J.; Pei, X.; Yu, J.; Guo, D. The complete plastid genome of *Cotinus coggygria* and phylogenetic analysis of the *Anacardiaceae*. *Genet. Mol. Biol.* **2021**, *44*, 3. [CrossRef] [PubMed]
25. Rossini, B.C.; de Moraes, M.L.T.; Marino, C.L. Complete chloroplast genome of *Myracrodruon urundeuva* and its phylogenetics relationships in *Anacardiaceae* family. *Physiol. Mol. Biol. Plants* **2021**, *27*, 801–814. [CrossRef] [PubMed]
26. Zarei, A.; Ebrahimi, A.; Mathur, S.; Lawson, S. The first complete chloroplast genome sequence and phylogenetic analysis of pistachio (*Pistacia vera*). *Diversity* **2022**, *14*, 577. [CrossRef]
27. Xu, Y.; Zhang, Y.; Ren, Z. Complete chloroplast genome of *Pistacia chinensis* Bunge (*Anacardiaceae*: Rhoideae), an important economical and ornamental plant. *Mitochondrial DNA Part B* **2020**, *5*, 1931–1932. [CrossRef]
28. Xu, Y.; Wen, J.; Su, X.; Ren, Z. Variation among the complete chloroplast genomes of the sumac species *Rhus chinensis*: Reannotation and comparative analysis. *Genes* **2022**, *13*, 1936. [CrossRef]
29. Barrett, C.F. Plastid genomes of the North American *Rhus integrifolia-ovata* complex and phylogenomic implications of inverted repeat structural evolution in *Rhus* L. *PeerJ* **2020**, *8*, e9315. [CrossRef]
30. Zong, D.; Qiao, Z.; Zhou, J.; Li, P.; Gan, P.; Ren, M.; He, C. Chloroplast genome sequence of triploid Toxicodendron vernicifluum and comparative analyses with other lacquer chloroplast genomes. *BMC Genom.* **2023**, *24*, 56. [CrossRef]

31. Doyle, J.J. A rapid DNA isolation procedure for small quantities of fresh leaf tissue. *Phytochem. Bull.* **1987**, *19*, 11–15.
32. Chen, Y.; Chen, Y.; Shi, C.; Huang, Z.; Zhang, Y.; Li, S.; Chen, Q. SOAPnuke: A MapReduce acceleration-supported software for integrated quality control and preprocessing of high-throughput sequencing data. *GigaScience* **2018**, *7*, gix120. [CrossRef] [PubMed]
33. Jin, J.J.; Yu, W.B.; Yang, J.B.; Song, Y.; de Pamphilis, W.C.; Yi, T.S.; Li, D.Z. GetOrganelle: A fast and versatile toolkit for accurate de novo assembly of organelle genomes. *Genome Biol.* **2020**, *21*, 241. [CrossRef] [PubMed]
34. Bankevich, A.; Nurk, S.; Antipov, D.; Gurevich, A.A.; Dvorkin, M.; Kulikov, A.S.; Lesin, V.M.; Nikolenko, S.I.; Pham, S.; Prjibelski, A.D.; et al. SPAdes: A new genome assembly algorithm and its applications to single-cell sequencing. *J. Comput. Biol.* **2012**, *19*, 455–477. [CrossRef] [PubMed]
35. Langmead, B.; Salzberg, S.L. Fast gapped-read alignment with Bowtie 2. *Nat. Methods* **2012**, *9*, 357–359. [CrossRef]
36. Camacho, C.; Coulouris, G.; Avagyan, V.; Ma, N.; Papadopoulos, J.; Bealer, K.; Madden, T.L. BLAST+: Architecture and applications. *BMC Bioinform.* **2009**, *10*, 421. [CrossRef]
37. Wick, R.R.; Schultz, M.B.; Zobel, J.; Holt, K.E. Bandage: Interactive visualization of de novo genome assemblies. *Bioinformatics* **2015**, *31*, 3350–3352. [CrossRef]
38. Liu, C.; Shi, L.; Zhu, Y.; Chen, H.; Zhang, J.; Lin, X.; Guan, X. CpGAVAS, an integrated web server for the annotation, visualization, analysis, and GenBank submission of completely sequenced chloroplast genome sequences. *BMC Genom.* **2012**, *13*, 715. [CrossRef]
39. Liu, S.; Ni, Y.; Li, J.; Zhang, X.; Yang, H.; Chen, H.; Liu, C. CPGView: A package for visualizing detailed chloroplast genome structures. *Mol. Ecol. Resour.* **2023**, *23*, 694–704. [CrossRef]
40. Nie, Z.L.; Sun, H.; Meng, Y.; Wen, J. Phylogenetic analysis of *Toxicodendron* (*Anacardiaceae*) and its biogeographic implications on the evolution of north temperate and tropical intercontinental disjunctions. *J. Syst Evol.* **2009**, *47*, 416–430. [CrossRef]
41. Angiosperm Phylogeny Group; Chase, M.W.; Christenhusz, M.J.; Fay, M.F.; Byng, J.W.; Judd, W.S.; Stevens, P.F. An update of the Angiosperm Phylogeny Group classification for the orders and families of flowering plants: APG IV. *Bot. J. Linn. Soc.* **2016**, *181*, 1–20. [CrossRef]
42. Zhang, D.; Gao, F.; Jakovlić, I.; Zou, H.; Zhang, J.; Li, W.X.; Wang, G.T. PhyloSuite: An integrated and scalable desktop platform for streamlined molecular sequence data management and evolutionary phylogenetic studies. *Mol. Ecol. Resour.* **2020**, *20*, 348–355. [CrossRef] [PubMed]
43. Kalyaanamoorthy, S.; Minh, B.Q.; Wong, T.K.F.; Haeseler, A.V.; Jermiin, L.S. ModelFinder: Fast model selection for accurate phylogenetic estimates. *Nat. Methods* **2017**, *14*, 587–589. [CrossRef] [PubMed]
44. Nguyen, L.T.; Schmidt, H.A.; von Haeseler, A.; Minh, B.Q. IQ-TREE: A fast and effective stochastic algorithm for estimating maximum-likelihood phylogenies. *Mol. Biol. Evol.* **2015**, *32*, 268–274. [CrossRef] [PubMed]
45. Minh, B.Q.; Nguyen, M.A.; von Haeseler, A. Ultrafast approximation for phylogenetic bootstrap. *Mol. Biol. Evol.* **2013**, *30*, 1188–1195. [CrossRef] [PubMed]
46. Ronquist, F.; Teslenko, M.; Van Der Mark, P.; Ayres, D.L.; Darling, A.; Höhna, S.; Larget, B.; Liu, L.; Suchard, M.; Huelsenbeck, J.P. MrBayes 3.2: Efficient Bayesian phylogenetic inference and model choice across a large model space. *Syst. Biol.* **2012**, *61*, 539–542. [CrossRef]
47. Bouckaert, R.; Vaughan, T.G.; Barido-Sottani, J.; Duchêne, S.; Fourment, M.; Gavryushkina, A.; Drummond, A.J. BEAST 2.5: An advanced software platform for Bayesian evolutionary analysis. *PLoS Comput. Biol.* **2019**, *15*, e1006650. [CrossRef]
48. Jiang, Y.; Gao, M.; Meng, Y.; Wen, J.; Ge, X.J.; Nie, Z.L. The importance of the North Atlantic land bridges and eastern Asia in the post-Boreotropical biogeography of the Northern Hemisphere as revealed from the poison ivy genus (*Toxicodendron*, *Anacardiaceae*). *Mol. Phylogenet. Evol.* **2019**, *139*, 106561. [CrossRef]
49. Manchester, S.R. Fruits and seeds of the middle Eocene Nut Beds flora, Clarno Formation, Oregon. *Palaeontogr. Am.* **1994**, *58*, 1–205.
50. MacGinitie, H.D. *Fossil Plants of the Florissant Beds*; Carnegie Institute: Washington, DC, USA, 1953.
51. Rambaut, A.; Drummond, A.J.; Xie, D.; Baele, G.; Suchard, M.A. Posterior summarisation in Bayesian phylogenetics using tracer 1.7. *Syst. Biol.* **2018**, *67*, 901–904. [CrossRef]
52. Katoh, K.; Standley, D.M. MAFFT multiple sequence alignment software version 7: Improvements in performance and usability. *Mol. Biol. Evol.* **2013**, *30*, 772–780. [CrossRef]
53. Rozas, J.; Ferrer-Mata, A.; Sánchez-DelBarrio, J.C.; Guirao-Rico, S.; Librado, P.; Ramos-Onsins, S.E.; Sánchez-Gracia, A. DnaSP 6: DNA sequence polymorphism analysis of large datasets. *Mol. Biol. Evol.* **2017**, *34*, 3299–3302. [CrossRef] [PubMed]
54. Leigh, J.W.; Bryant, D. POPART: Full-feature software for haplotype network construction. *Methods Ecol. Evol.* **2015**, *6*, 1110–1116. [CrossRef]
55. Frazer, K.A.; Pachter, L.; Poliakov, A.; Rubin, E.M.; Dubchak, I. VISTA: Computational tools for comparative genomics. *Nucleic Acids Res.* **2004**, *32*, 273–279. [CrossRef]
56. Darling, A.E.; Mau, B.; Perna, N.T. progressiveMauve: Multiple genome alignment with gene gain, loss and rearrangement. *PLoS ONE* **2010**, *5*, e11147. [CrossRef]
57. Kearse, M.; Moir, R.; Wilson, A.; Stones-Havas, S.; Cheung, M.; Sturrock, S.; Buxton, S.; Cooper, A.; Markowitz, S.; Duran, C.; et al. Geneious Basic: An integrated and extendable desktop software platform for the organization and analysis of sequence data. *Bioinformatics* **2012**, *28*, 1647–1649. [CrossRef]

58. Amiryousefi, A.; Hyvönen, J.; Poczai, P. IRscope: An online program to visualize the junction sites of chloroplast genomes. *Bioinformatics* **2018**, *34*, 3030–3031. [CrossRef] [PubMed]
59. Kurtz, S.; Choudhuri, J.V.; Ohlebusch, E.; Schleiermacher, C.; Stoye, J.; Giegerich, R. REPuter: The manifold applications of repeat analysis on a genomic scale. *Nucleic Acids Res.* **2001**, *29*, 4633–4642. [CrossRef]
60. Benson, G. Tandem repeats finder: A program to analyze DNA sequences. *Nucleic Acids Res.* **1999**, *27*, 573–580. [CrossRef]
61. Beier, S.; Thiel, T.; Münch, T.; Scholz, U.; Mascher, M. MISA-web: A web server for microsatellite prediction. *Bioinformatics* **2017**, *33*, 2583–2585. [CrossRef]
62. Thiel, T.; Michalek, W.; Varshney, R.; Graner, A. Exploiting EST databases for the development and characterization of gene-derived SSR-markers in barley (*Hordeum vulgare* L.). *Theor. Appl. Genet.* **2003**, *106*, 411–422. [CrossRef]
63. Hall, T.A. BioEdit: A user-friendly biological sequence alignment editor and analysis program for windows 95/98/NT. *Nucleic Acids Symp. Ser.* **1999**, *41*, 95–98.
64. Wang, L.; He, N.; Li, Y.; Fang, Y.M.; Zhang, F.L. Complete chloroplast genome sequence of Chinese lacquer tree (*Toxicodendron vernicifluum*, *Anacardiaceae*) and its phylogenetic significance. *BioMed Res. Int.* **2020**, *2020*, 9014873. [CrossRef] [PubMed]
65. Zhong, Y.; Zong, D.; Zhou, A.; He, X.F.; He, C.Z. The complete chloroplast genome of the *Toxicodendron vernicifluum* cv. Dahongpao, an elite natural triploid lacquer tree. *Mitochondrial DNA B* **2019**, *4*, 1227–1228. [CrossRef]
66. He, N.; Wang, L.; Li, Y.; Fang, Y.; Zhang, F. The complete chloroplast genome sequence of *Toxicodendron sylvestre* (*Anacardiaceae*). *Mitochondrial DNA Part B* **2020**, *5*, 2008–2009. [CrossRef]
67. Wicke, S.; Schneeweiss, G.M.; dePamphilis, C.W.; Müller, K.F.; Quandt, D. The evolution of the plastid chromosome in land plants: Gene content, gene order, gene function. *Plant Mol. Biol.* **2011**, *76*, 273–297. [CrossRef] [PubMed]
68. Hohmann, N.; Wolf, E.M.; Rigault, P.; Zhou, W.; Kiefer, M.; Zhao, Y.; Koch, M.A. *Ginkgo biloba*'s footprint of dynamic Pleistocene history dates back only 390,000 years ago. *BMC Genom.* **2018**, *9*, 299. [CrossRef]
69. Renoult, J.P.; Kjellberg, F.; Grout, C.; Santoni, S.; Khadari, B. Cyto-nuclear discordance in the phylogeny of *Ficus* section Galoglychia and host shifts in plant-pollinator associations. *BMC Evol. Biol.* **2009**, *9*, 248. [CrossRef]
70. Luo, D.; Xu, B.; Li, Z.M.; Sun, H. Biogeographical divides delineated by the three-step landforms of China and the East China Sea: Insights from the phylogeography of *Kerria japonica*. *J. Biogeogr.* **2021**, *48*, 372–385. [CrossRef]
71. Wang, W.; Chen, S.; Zhang, X. Whole-genome comparison reveals heterogeneous divergence and mutation hotspots in chloroplast genome of *Eucommia ulmoides* Oliver. *Int. J. Mol. Sci.* **2018**, *19*, 1037. [CrossRef]
72. Park, I.; Yang, S.; Kim, W. Sequencing and comparative analysis of the chloroplast genome of *Angelica polymorpha* and the development of a novel indel marker for species identification. *Molecules* **2019**, *24*, 1038. [CrossRef]
73. Huang, Y.; Wang, J.; Yang, Y. Phylogenomic analysis and dynamic evolution of chloroplast genomes in Salicaceae. *Front. Plant Sci.* **2017**, *8*, 1050. [CrossRef] [PubMed]
74. Liu, W.; Kong, H.; Zhou, J. Complete chloroplast genome of *Cercis chuniana* (*Fabaceae*) with structural and genetic comparison to six species in Caesalpinioideae. *Int. J. Mol. Sci.* **2018**, *19*, 1286. [CrossRef] [PubMed]
75. Zhu, A.; Guo, W.; Gupta, S. Evolutionary dynamics of the plastid inverted repeat: The effects of expansion, contraction, and loss on substitution rates. *New Phytol.* **2016**, *209*, 1747–1756. [CrossRef] [PubMed]
76. Weng, M.L.; Blazier, J.C.; Govindu, M.; Jansen, R.K. Reconstruction of the ancestral plastid genome in Geraniaceae reveals a correlation between genome rearrangements, repeats, and nucleotide substitution rates. *Mol. Biol. Evol.* **2014**, *31*, 645–659. [CrossRef] [PubMed]